Electron Spin Resonance

Eric Reichwein
Bryce Burgess
Department of Physics
University of California, Santa Cruz

February 24, 2014

Abstract

We studied electron spin resonance in diphenyl-picril-hydrazyl (DPPH). We chose DPPH for the one unpaired free radical (free electron). Using a reflex klystron we produced microwave radiation measured the interference of signal that was purely reflected and a signal that was reflected (or absorbed) by DPPH. We determined the radiation frequency to be $\nu = 9.253\,\mathrm{GHz}$. The external magnetic field had some hysteresis effect. During the up swing resonance occurred when $B_{ext} = 3201 \pm 1 Gauss$ and on the down swing resonance occurred when $B_{ext} = 3199 \pm 1 Gauss$. From here we used semi-classical mechanics to derive the Lande g-factor to be $g = 2.0659 \pm 0.0655$ which was about 3% of the established value of $g = 2.0036$.

Contents

1 Introduction

We examined the electron spin resonance (ESR) of the chemical compound diphenyl-picril-hydrazyl (DPPH), as seen in Fig. 1. Using a klystron to generate microwave radiation we looked at interference of simply reflected radiation and the reflection of the radiation off of the DPPH. Due to the nature of DPPH, the microwave radiation gets absorbed at single frequency, which we call resonance. DPPH is unique because it has zero angular momentum, and a free valence electron, which will indeed interact with the magnetic field. [1]

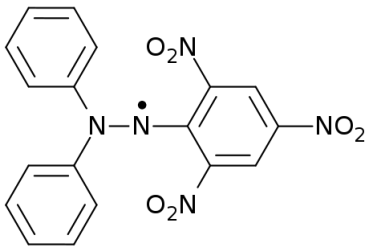

Figure 1: The chemical structure of DPPH. Note the free electron (or free radical) on the center nitrogen.

1.1 Historical Background

The ESR is complicated phenomena that has many layers and aspects to it which we will briefly outline here.

1.1.1 Zeeman Effect

In 1896, Pieter Zeeman disobeyed his superior and used the laboratory to measure the splitting of spectral lines of a substance placed in a magnetic field. This splitting has to due with the interaction between the magnetic moment of the electrons and the magnetic field. Pieter Zeeman and Hendrik Lorentz won the 1902 Nobel Prize for this discovery. The magnetic moment is inherently tied to the concept of the electron spin, which was first observed in 1921 with one of the most famous experiments in modern physics.[2]

1.1.2 Stern-Gerlach Experiment

Otto Stern and Walther Gerlach devised an experiment to measure the quantization of orbital angular momentum of the Bohr model of atoms. They used silver atoms because they believed silver atoms had angular momentum $\ell = 1$, which was actually wrong.[1] If silver had angular momentum of $\ell = 1$ then the beam should have split into three components (for the $\ell = 0, \pm 1$ cases) as it passed through the inhomogeneous magnetic field. However, it split into two

[1]Silver actually has angular momentum $\ell = 0$, but Stern-Gerlach did not know that because they were operating under Bohr-Sommerfeld thoery. For more in depth discussion vist: plato.stanford.edu/entries/physics-experiment/app5.html.

beams for the $s = \pm 1/2$ intrinsic angular momentum of electron spins. The original beam record is shown in Fig. 2. It would take 4 years to reconcile this perplexing result. [4]

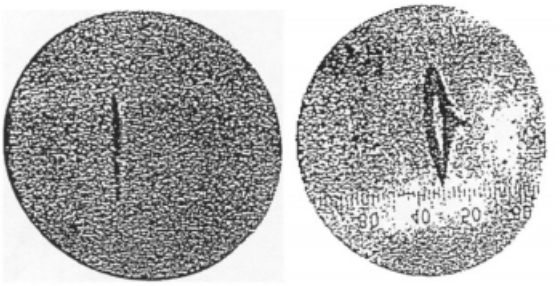

Figure 2: The photographic plate of Stern-Gerlach experiment. The left is of the zero magnetic field and the right shows when an inhomogeneous magnetic field is applied.

1.1.3 Uhlenbeck-Goudsmit Postulate of Spin and The Dirac Equation

Uhlenbeck and Goudsmit proposed that electrons have the "intrinsic angular momentum" or spin which would interact with the magnetic fields through the magnetic moment.[5] There is no shape or size to an electron which makes the fact that this intrinsic property seem as if does was (and still is) very perplexing. They proposed the spin is quantized in the same way as the angular momentum, namely,

$$S_z = m_s \hbar \tag{1}$$

Where S_z is the spin angular momentum in the z direction, m_s is the quanta ($m_s = \pm 1/2, \pm 3/2...$ for fermions), and *hbar* is Planck's constant and has units of angular momentum.

In 1928, Dirac came along and explained this property in his derivation of the relativistic wave equation. His theory is much too advanced to talk about here, but just note that his theory was in accordance with Uhlenbeck and Goldsmits postulate and the Stern-Gerlach experiment. [5]

1.1.4 First Observation of ESR and Applications

In 1945 Russian physicist Yevgeny Zavoisky measured the first ESR in $CuCl{\cdot}2H_20$. His work was inspired by Rabi's work on energy level transitions caused by oscillating electromagnetic fields. It is rumored that he actually discovered nuclear magnetic resonance 5 years before Bloch and Purcell did in 1946 and later won a Nobel Prize for.

Electron spin resonance, commonly referred to electron paramagnetic resonance, is used for locating dangling covalent bonds and paramagnetic centers (i.e. crystallographic defects where electrons are bunched together instead of atom). This has many more applications in material science, biology, chemistry, etc. Now that we know a little about the history of ESR, we can discuss the physics behind this extraordinary phenomena.

1.2 Physics of ESR

The main point of this lab is measure the dimensionless Lande g factor. This is a quantity inherently tied to quantum mechanics (specifically quantum electrodynamics). It arises from the fact the electron has the intrinsic angular momentum called spin. Due to this property the electron also has a magnetic moment μ, which is anti-parallel to the spin vector.[6] The magnetic moment in the z direction is given in relation to Eq. 1 as

$$\mu_z = g\left(\frac{q}{2m_e}\right)S_z = g\left(\frac{q}{2m_e}\right)m_s\hbar = g\mu_b m_s \tag{2}$$

Where $\mu_b = (q\hbar/2m_e)$ is called the Bohr Magneton. Going further and recalling the potential energy between a magnetic field and magnetic moment ,$U = -\mu \cdot B$, we can calculate the energy difference between the two quantum states (namely, spin parallel and antiparallel to external magnetic field),

$$U = -\mu_z \cdot B = -g\mu_b m_s B\cos\theta \tag{3}$$

And now we look at the energy difference,

$$\begin{aligned}\Delta U &= -g\mu_b m_s B\cos(\pi) - (-g\mu_b m_s B\cos(0)) \\ &= 2g\mu_b m_s B \\ &= g\mu_b B\end{aligned} \tag{4}$$

Where in the last step we invoked the condition of $m_s = 1/2$ and we have handled its sign previously in the derivation. Now we can probe this quantized energy difference by shooting photons with energy that are precisely equal to the energy difference of the quantum states. If we apply a magnetic field the electrons will tend to align themselves parallel to the magnetic field because that is the low energy state. The photons will be absorbed by the electrons and flip the electron to the higher energy state. This only happens at a very precise photon energy (or frequency). We can determine what frequency this needs to be at by equating the the change in electron energy to photon energy,

$$\begin{aligned}E &= \hbar\omega \\ &= \Delta U \\ &= g\mu_b B\end{aligned}$$

Therefore,

$$\omega = \frac{g\mu_b B}{\hbar} = \frac{gqB}{2m_e} \tag{5}$$

Equation 5 tells us resonant frequency of the klystron (and consequently the photons) to observe electron spin resonance in DPPH. Once we determine this we can conclude what the Lande g factor is by rearranging Eq. 5,

$$\omega = \frac{gqB}{2m_e} \longrightarrow g = \frac{2m_e\omega}{qB} \tag{6}$$

2 Procedures and Setup

The bulk of this experiment was based on the setup and tuning of the apparatus so we shall spend a good portion of this lab report describing the setup in detail. In Fig. 3 we have labeled each part of the apparatus in numerical order of the power propagation.

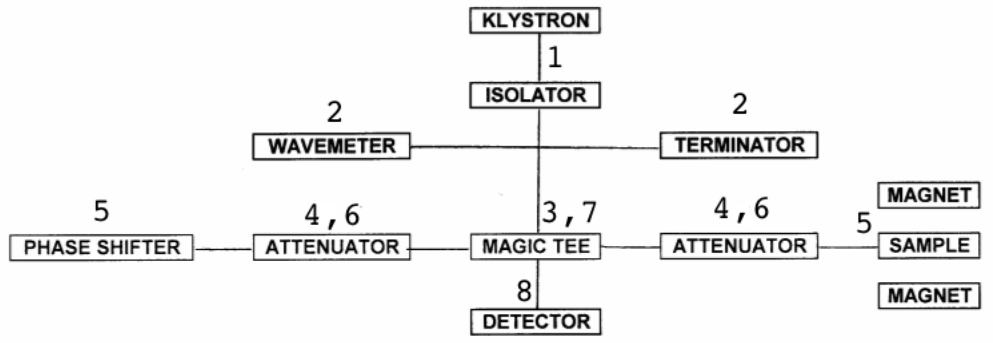

Figure 3: The schematic of the ESR apparatus.

2.1 The Reflex Klystron (1) and Isolator (1)

The reflex klystron is an oscillator amplifier. It produces the electronic oscillations that produce the power output and ultimately the photons. In Fig. 4 it shows electrons being accelerated towards a negatively charged plate after passing through a resonance chamber. They will be "reflected" by this plate and return back to where they came from. It is in this return path when they get bunched together.[2] It is in the second time going through the resonant chamber that these electron bunches produce an output signal.

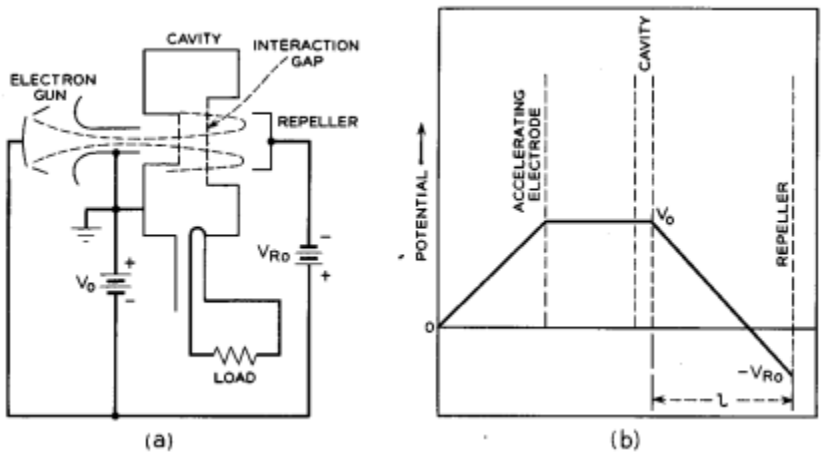

Figure 4: The reflex klystron. (a) The schematic of the klystron (b) The potential profile from cathode to repeller.[7]

[2]The word klystron comes from the german word klystern which means "bunching".

This signal also modulates the electrons velocity the first time they pass through the resonant chamber as well. The output signal gets picked up through charge accumulation on the resonant chamber walls, this then gets transferred through to the load and pickup loop (the load and chamber circuit can be thought of equivalently as a voltage and current source and a LRC circuit.) By tuning the load (and it equivalent circuit) we get that a resonance of the circuit and hence the largest power output. The pickup loop is then sent to an antenna which produces the microwave radiation.

Once the microwave radiation has been produced by the klystron, it is then passed through the isolator. The isolator is made from the chemical compound ferrite (of mainly iron oxides i.e. Fe_2O_3). Ferrite along with a rotating magnetic field allow for the passing of the power in one direction but not in the reverse.

2.2 The Wave Meter (2) and Terminator (2)

The microwave frequency radiation then hits a "tee" which splits the power into two unequal parts. The small part gets diverted into the wave meter. This is a resonant cavity that will measure the frequency of the radiation and calibrate the klystron. It accomplishes this by finely tuning the size the of the cavity to obtain maximum resonance which is picked up by the crystal detector.

During the "tee" splitting some radiation gets split in the opposite direction of the wave meter. This radiation is merely absorbed by material in the terminator to prevent it from interfering with the main beam.

2.3 The Magic Tee (3,7)

The magic tee has four ports and output. The first two ports split the input (from klystron) into two equal beams. One goes toward the sample and one goes towards the phase shifter. On the return back to the tee the beams go into another port (one for each beam) and get directed to the diode detector. The reason they don't go back into the port they came from is that there is an isolator type device that prevents back flow of power that would create interference and attenuation of the signal. [3]

2.4 The Attenuator (4,6) and Phase Shifter (5)

The attenuator is essentially a piece of material that absorbs a small fraction of the photons. This device allows for essentially no reflection of signal. If signal were reflected it would cause significant signal attenuation and interference. Once the radiation passes through the attenuator it is reflected by the phase shifter. To change the phase of the radiation we just adjust the distance from the magic tee. For example if we adjusted the distance to be a quarter wavelength farther than the sample distance. Then the radiation would be half a wavelength out of phase corresponding to half a wavelength farther in distance it has to travel (half wavelength is because extra quarter wavelength there and an extra quarter wavelength back). We adjust these devices to make the signal down this arm equivalent to the signal coming from the sample. This calibration makes the final signal maximum for resonance and essentially zero if we are off resonance. [3]

2.5 The Sample and Magnet (5)

After the beam is split at the magic tee, it heads to the sample (after first passing through an attenuator). The smaple is in a rectangular wave guide, to direct the beam to the sample efficiently. The sample as noted in the introduction is DPPH. We chose DPPH because it has one free electron with no orbital angular momentum and it also has very diffuse unpaired spins which make the line widths very small. [1] The magnet is the standard Helmholtz coils with some permanent magnets to confine the magnetic field to the inner region. For the magnetic fields we are probing we used a hall probe.

2.6 The Diode Detector (8)

The detector is a diode placed in the waveguide at the point of maximum electric field. [3] This electric field reduces the effective resistance of the diode and current begins to flow. The flow of current is then amplified even more and sent to the oscilloscope. The current is inversely proportional to the temperature squared and proportional to the radiation voltage, refer to the lab manual for more details[3]

3 Data and Analysis

We present our data, which is mainly in the form of oscilloscope plots. Some other data was recorded directly from the signal generators, magnetic field sources, and hall probe devices and is summarized below.

3.1 The Wave Meter Q Factor

We measured the wave meter resonant frequency to be 9.256 GHz with a width of approximately 50 ± 10 kHz. The quality factor is then

$$Q = \frac{\omega}{\Delta\omega} = \frac{9.256\,\text{GHz}}{50.000\,\text{Hz}} = 1.8 \times 10^6 \pm 0.2 \times 10^6 \tag{7}$$

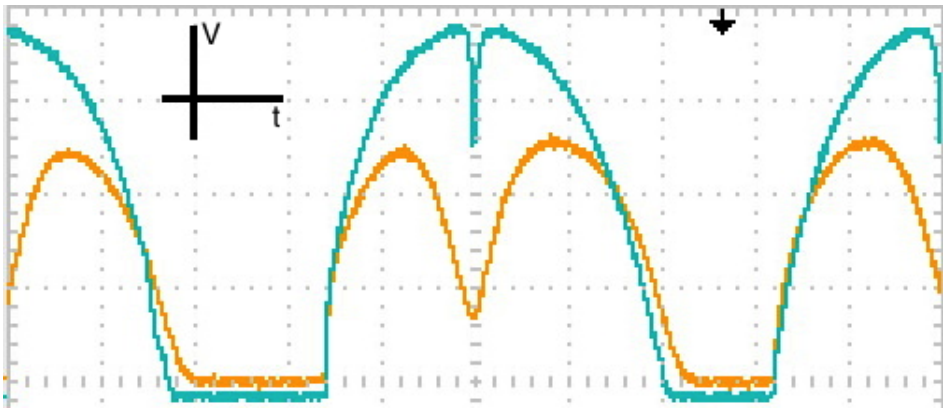

Figure 5: Oscilloscope readout of crystal detector and diode detector.

In Fig. 5 we observe the wave meter crystal detector signal (larger amplitude, blue) and the diode detector signal (smaller amplitude, yellow). We expect the wave meter to have a higher Q factor than the $Q = 100$ klystron resonant cavity. Comparing the two widths we see that the klystron is indeed roughly 10^4 times wider than the wave meter Q (note the scale difference).

3.2 Rectangular Wave Guide Cut Off Frequency Calculations

The waveguides are essential in this experiment because it allows for strongly collimated and direct radiation with very low power loss. We present here some waveguide calculations of resonant frequencies presented in the table below. We will show the lowest frequency calculation and the rest of the values are merely presented in the table. Waveguide calculations are derived from applying Maxwell's equations with the proper boundary conditions to the shape of the waveguide. For instance, we are using hollow conductive rectangular waveguides. The waveguide used here produce transverse electric field (TE) transmission. This means that $E_z = 0$ and $B_z \neq 0$, or that the electric field oscillates entirely orthogonal to the direction of power propagation. For any waveguide there is a cutoff frequency in which below the minimum value no power propagation can occur. Above the minimum cutoff frequency there are only certain modes that can propagate power. The lowest cutoff frequency needs to be near the desired frequency of the radiation, or in lay terms we need a specific bandwidth. Otherwise too many modes of radiation propagate through the waveguide and can create interference and attenuation problems. From solving the Maxwell equations with proper boundary conditions, which we will omit, we obtain the formula (Eq. 8) for the cutoff frequency.

$$f_{mn} = \frac{c}{2}\left[\left(\frac{m}{a}\right)^2 + \left(\frac{n}{b}\right)^2\right]^{1/2} \tag{8}$$

Where c is the speed of light, a and b are waveguide dimensions, and m and n are integers corresponding to the particular mode. The lowest mode is the TE_{10}, with $a = 0.004'' = 0.00010m$ and $b = 0.009'' = 0.00023m$

$$\begin{aligned}
f_{mn} =& \frac{c}{2}\left[\left(\frac{n}{a}\right)^2 + \left(\frac{m}{b}\right)^2\right]^{1/2} \\
f_{10} =& \frac{c}{2}\left[\left(\frac{1}{0.0001m}\right)^2 + \left(\frac{0}{0.00023m}\right)^2\right]^{1/2} \\
f_{10} =& \frac{c}{2(0.0001m)} \\
f_{10} =& 6.523\,\mathrm{GHz}
\end{aligned}$$

This is the absolute lowest cutoff frequency. The next 4 highest ones (note there is no degeneracy because in most cases $a \neq b$) are presented in Table 1 below.

Table 1: Wave Guide Cutoff frequencies

Mode	frequency
TE_{10}	6.523 GHz
TE_{01}	15.00 GHz
TE_{11}	163.6 GHz
TE_{12}	198.8 GHz
TE_{21}	307.7 GHz
TE_{22}	328.0 GHz

For the waveguide resonant cavity with the sample we can approximate as solid rectangular box with no apertures. Solving Maxwell's equations with the appropriate boundary conditions gives us (Eq. 9) the following cutoff frequency relation

$$f_{\ell mn} = \frac{c}{2}\left[\left(\frac{\ell}{a}\right)^2 + \left(\frac{m}{b}\right)^2 + \left(\frac{n}{d}\right)^2\right]^{1/2} \tag{9}$$

Where c is the speed of light, a, b, and d are waveguide cavity dimensions, and ℓ, m and n are integers corresponding to the particular mode. The lowest mode is the TE_{001}, with $a = 0.004'' = 0.00010m$, $b = 0.009'' = 0.00023m$ and $d = 1.543'' = 0.0393m$. We will omit the trivial calculations of these modes but merely present them in Table 2 below.

Table 2: Wave guide resonant cavity cutoff frequencies

Mode	frequency
TE_{100}	15.00 GHz
TE_{010}	6.523 GHz
TE_{001}	0.0383 GHz
TE_{110}	16.36 GHz
TE_{101}	15.00 GHz
TE_{011}	6.523 GHz
TE_{111}	16.36 GHz

From Table 2 we see that really only two modes dominant in resonant cavity: the TE_{010} an the TE_{011}. This is because of the relatively large d value. They are approximately the same cutoff frequency so we now there wont be any noticeable interference or attenuation.

3.3 Determination of Lande g-Factor

Using Eq. 6 we can determine the g-factor. We swept the current of the Helmholtz coil and varied the magnetic field between $2000 Gauss$ to $4000 Gauss$. We observed an hysteresis effect. In Fig. 6 we show the hysteresis effect on the oscilloscope. In Fig.7 we show essentially the same thing except that we used a differentiator filter to obtain higher precision.

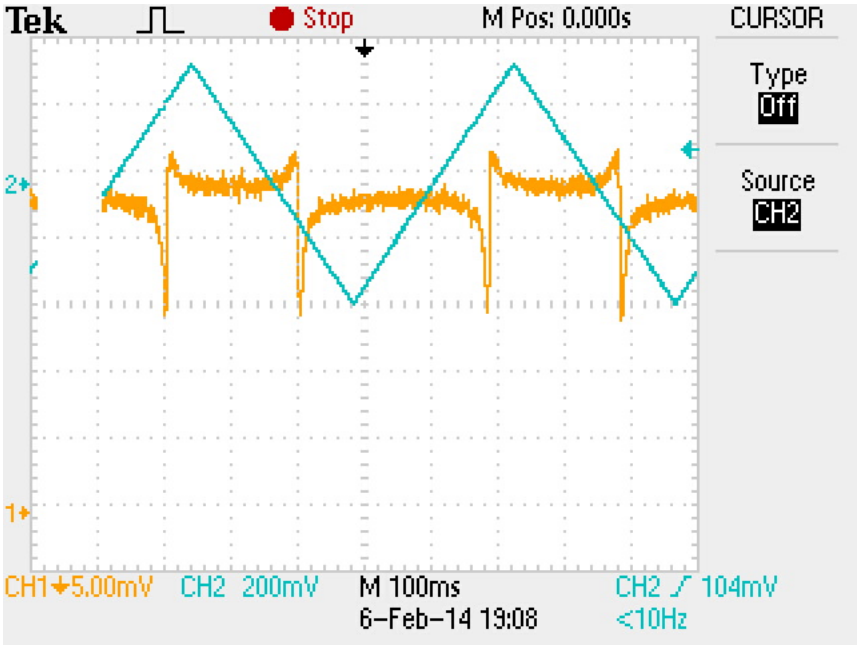

Figure 6: Oscilloscope readout of the sweeping signal (magnetic field) and diode detector.

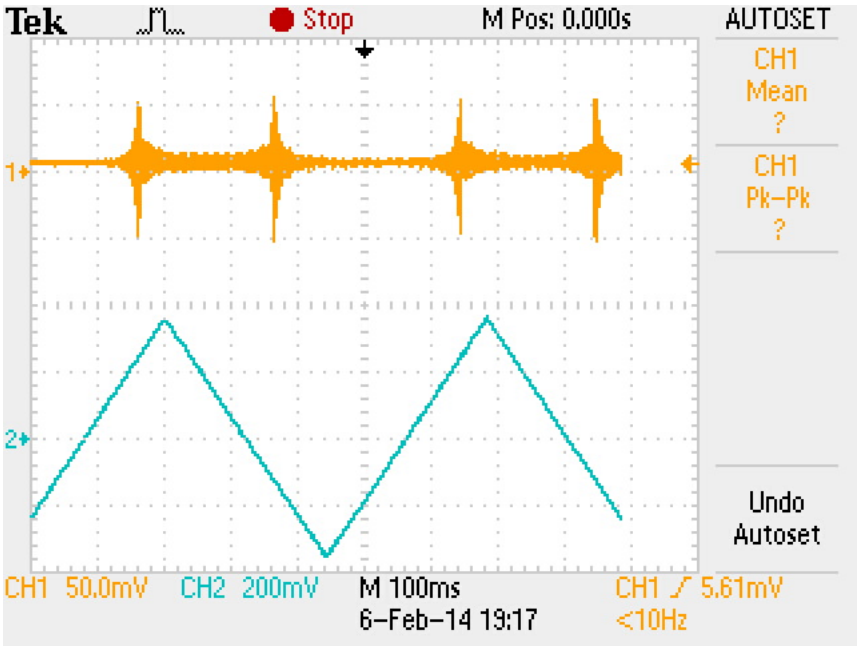

Figure 7: Oscilloscope readout of the differentiated sweeping signal (magnetic field) and diode detector.

During the up sweep we observed resonance at $3201 \pm 1 Gauss$ and on the down sweep we

observed 3199±1$Gauss$. The upswing g factor calculation is

$$\begin{aligned} g =& \frac{2m_e\omega}{e^- B} \\ g =& \frac{4\pi m_e \nu}{e^- B} \\ =& \frac{4\pi(9.10938 \times 10^{-31} kg)9.256\,\text{GHz}}{(1.60218 \times 10^{-19})3201 Gauss} \\ =& 2.0653 \end{aligned}$$

On the down swing we have

$$\begin{aligned} g =& \frac{2m_e\omega}{e^- B} \\ g =& \frac{4\pi m_e \nu}{e^- B} \\ =& \frac{4\pi(9.10938 \times 10^{-31} kg)9.256\,\text{GHz}}{(1.60218 \times 10^{-19})3199 Gauss} \\ =& 2.0665 \end{aligned}$$

Combining these two results we find that the average is

$$g = (2.0665 + 2.0653)/2 = 2.0659$$

Comparing this result to the established value of $g = 2.0032$ we find that we are within approximately 3% of the true value.

4 Conclusion

The majority of the experiment was based on calibration of the signals and detectors. We left out the calibration procedures for clarity purposes. We used microwave radiation to observe electron spin resonance. The resonance we refer to is maximum absorption of radiation by the spin state of the electron. When an external magnetic field is applied the unpaired electron (of the DPPH molecule) is in its lowest energy state. The radiation then excited the electron to it's higher energy state and there was significantly was less signal.

The laboratory manual was, in my opinion, poorly written. We ran into a lot of problems after deciphering the lab manual incorrectly multiple times. This put us behind schedule and took away from our analysis time. The lab manual also gives a very vague and misleading description of the physics of the equipment especially the reflex klystron, isolator and attenuator. The equipment is very old and we were unable to find any data sheets or specification sheets on the equipment. There were some points that I felt the lab manual needed a diagram (or at least a better one) which would compliment the descriptions.

This experiment was mainly focused on the setup portion, which is very practical and informative. The analysis required only a few well known simple calculations, which was not very informative. I wish we had spent more time on the error analysis, and in the next draft of the report we will include more detailed error calculations.

References

[1] Dunn, E.K. ESR of DPPH, 2011. University of Kansas.

[2] https://physics.ucsd.edu/students/courses/spring2012/physics4e/zeemaneffect.pdf

[3] George Brown, Sue Carter. Physics 134 Lab Manual. Winter 2014.

[4] http://plato.stanford.edu/entries/physics-experiment/app5.html. Stanford Encyclopedia.

[5] http://www.lorentz.leidenuniv.nl/history/spin/goudsmit.html

[6] Weil, John and Bolton, James. Electron Paramagnetic Resonance. 2007.

[7] Principles of Electron Tubes, Including Grid-Controlled Tubes, Microwave Tubes and Gas Tubes. J. W. Gewartowski and H. A. Watson. Bell Telephone Laboratories 1965